Comparisons of HRD and SLOSH Surface Wind Fields in Hurricanes: Implications for Storm Surge Modeling

SAMUEL H. HOUSTON

Hurricane Research Division, NOAA/AOML, Miami, Florida

WILSON A. SHAFFER

Techniques Development Laboratory, NOAA/NWS/OSD, Silver Spring, Maryland

MARK D. POWELL

Hurricane Research Division, NOAA/AOML, Miami, Florida

JYE CHEN

Techniques Development Laboratory, NOAA/NWS/OSD, Silver Spring, Maryland

(Manuscript received 10 October 1998, in final form 4 March 1999)

ABSTRACT

Surface wind observations analyzed by the Hurricane Research Division (HRD) were compared to those computed by the parametric wind model used in the National Weather Service Sea, Lake, and Overland Surges from Hurricanes (SLOSH) model's storm surge computations for seven cases in five recent hurricanes. In six cases, the differences between the SLOSH and HRD surface peak wind speeds were 6% or less, but in one case (Hurricane Emily of 1993) the SLOSH computed peak wind speeds were 15% less than the HRD. In all seven cases, statistics for the modeled and analyzed wind fields showed that for the region of strongest winds, the mean SLOSH wind speed was 14% greater than that of the HRD and the mean inflow angle for SLOSH was 19° less than that of the HRD. The radii beyond the region of strongest winds in the seven cases had mean wind speed and inflow angle differences that were very small. The SLOSH computed peak storm surges usually compared closely to the observed values of storm surge in the region of the maximum wind speeds, except Hurricane Emily where SLOSH underestimated the peak surge. HRD's observation-based wind fields were input to SLOSH for storm surge hindcasts of Hurricanes Emily and Opal (1995). In Opal, the HRD input produced nearly the same computed storm surges as those computed from the SLOSH parametric wind model, and the calculated surge was insensitive to perturbations in the HRD wind field. For Emily, observation-based winds produced a computed storm surge that was closer to the peak observed surge, confirming that the computed surge in Pamlico Sound was sensitive to atmospheric forcing. Using real-time, observation-based winds in SLOSH would likely improve storm surge computations in landfalling hurricanes affected by synoptic and mesoscale factors that are not accounted for in parametric models (e.g., a strongly sheared environment, convective asymmetries, and stably stratified boundary layers). An accurate diagnosis of storm surge flooding, based on the actual track and wind fields could be supplied to emergency management agencies, government officials, and utilities to help with damage assessment and recovery efforts.

1. Introduction

As the populations of coastal areas grow, more lead time is required to safely evacuate people from the dangers posed by hurricane storm surge (Jarrell et al. 1992). The Sea, Lake, and Overland Surges from Hurricanes (SLOSH) model (Jelesnianski et al. 1992), developed by the National Weather Service's (NWS) Techniques Development Laboratory (TDL), provides the primary guidance used by emergency management officials to develop and carry out coastal evacuation plans. Jarvinen and Lawrence (1985) compared 523 storm surge height observations (i.e., tide gauge measurements and high water marks from the interior of buildings) to SLOSH hindcast values in 10 hurricanes, finding a 0.43-m mean absolute error with a standard deviation of 0.61 m and a bias of −0.09 m. This level of documented performance has made SLOSH the primary tool for the Federal Emergency Management Agency's (FEMA) evacuation

Corresponding author address: Sam Houston, HRD/AOML/NOAA, 4301 Rickenbacker Causeway, Miami, FL 33149.
E-mail: houston@aoml.noaa.gov

studies (V. Wiggert, Hurricane Research Division, 1998, personal communication). The track forecasts of the Tropical Prediction Center's (TPC) National Hurricane Center (NHC) have a mean error of 177 km within 24 h of landfall (McAdie and Lawrence 1993). This 177-km region of uncertainty near a coastline requires issuing warnings and commencing evacuations over a large region at least 24 h in advance of landfall. As part of comprehensive hurricane evacuation studies funded by FEMA, SLOSH is used to map the storm surge flood plain in each of 40 U.S. SLOSH basins. Atlases of storm surge flooding are created for each basin based on climatologically likely storm directions, speeds, intensities, and sizes. One such composite is the maximum envelope of water (MEOW), which depicts the highest surges from a family of individual runs, all having the same intensity, forward speed, and landfall direction, but varying in landfall location. These MEOWs are available in advance to emergency managers and others who need to make decisions about evacuations of coastlines that may potentially be impacted by hurricane storm surge.

Modeling technologies for estimating storm surge near the coast require realistic atmospheric forcing in tropical cyclones. SLOSH was designed to allow storm surge computations to be made with limited knowledge of the storm's structure and intensity and to avoid uncertainties associated with input fields derived from hurricane wind measurements. SLOSH incorporates topography, channels, and barriers, and computes overland flooding, but it does not include wave runup, wave setup, or flooding from rainfall (note that initial tide levels or astronomical tides can be added to the model results). Simple parametric wind models can force storm surges for generic hurricanes, but the computed winds can differ significantly from the hurricane's actual wind field when the parameters are poorly specified or insufficient. For example, the convection from Hurricane Emily's (1993) western eyewall crossed eastern Pamlico Sound in North Carolina and caused very strong surface winds on the left side of the northward moving hurricane (Burpee et al. 1994). Therefore, SLOSH's parametric wind model could not correctly compute Emily's nearly symmetric wind field. In addition, the model uses *lake winds* over bays and inland lakes to account for the greater friction associated with marine wind trajectories affected by land (Jelesnianski et al. 1992; Houston and Powell 1994). These winds have more inflow and weaker wind speeds than oceanic SLOSH winds. In Emily, SLOSH significantly underestimated the surface winds and the resulting storm surge observed on the Pamlico Sound side of Cape Hatteras.

Recently, the National Oceanic and Atmospheric Administration (NOAA) Hurricane Research Division (HRD) and TDL have compared observation-based tropical cyclone wind fields to those computed by the SLOSH model. Houston and Powell (1994) compared observed and simulated winds, storm surges, and water-level time series for Tropical Storm Marco (1990) and found that SLOSH reasonably represented the wind fields and storm surges in two basins (i.e., two individual SLOSH model domains) having relatively complicated coastlines. A similar comparison was made for Hurricane Andrew's (1992) landfall in south Florida (Powell and Houston 1996, hereafter called PH96), which concluded that HRD's real-time wind field information might be useful for improving storm surge and wave model initializations and forecasts. Boundary layer and surface wind observations in the hurricane's inner core have been very scarce in the past, but the advent of new technologies, such as the Global Positioning System (GPS) dropwindsondes described by Hock and Franklin (1999), are changing this. The dropwindsondes are capable of making measurements in the boundary layer and at the surface in the hurricane's eyewall. The HRD wind fields, which can be considered state-of-the-art representations of the surface winds in hurricanes, are capable of including these and other future surface observations (e.g., drifting buoys) from the hostile environment of the hurricane's inner core.

This paper compares SLOSH and HRD surface wind fields for Hurricanes Hugo (1989), Bob (1991), Andrew (1992), Emily (1993), and Opal (1995). Each hurricane caused a significant storm surge by making landfall or approaching the U.S. shoreline (Fig. 1). A storm history reference for each hurricane is listed in Table 1. The observation-based HRD winds are assumed representative of each storm's ''true'' surface wind field and were used to validate the SLOSH parametric wind modeling approach. The methodology used to produce SLOSH and HRD winds is described in section 2. Section 3 compares the SLOSH and HRD winds and section 4 shows the impact of HRD wind fields on the SLOSH model for two hurricanes. Discussion and concluding remarks are provided in section 5.

2. Methodology

a. SLOSH parametric wind model

The SLOSH parametric wind model is described by Jelesnianski et al. (1992) and Houston and Powell (1994). ''Snapshots'' of the two-dimensional SLOSH model wind fields were created for the present study. Model input parameters include the storm's track (which provides translational motion for a 72-h period), radius of maximum winds (R_{MW}), and pressure deficit (Δp; e.g., the value of Δp is 6.1 kPa if the environmental pressure is 101.0 kPa and the hurricane's central pressure is 94.9 kPa). SLOSH was designed to allow parameters to vary at 1-h intervals but is usually run with a 6-h interval. SLOSH input parameters for the seven landfall snapshots of surface wind fields are listed in Table 2. The R_{MW} was normally based on published reports, except in the case of Emily and Bob where the values of R_{MW} were determined from surface and aircraft observations.

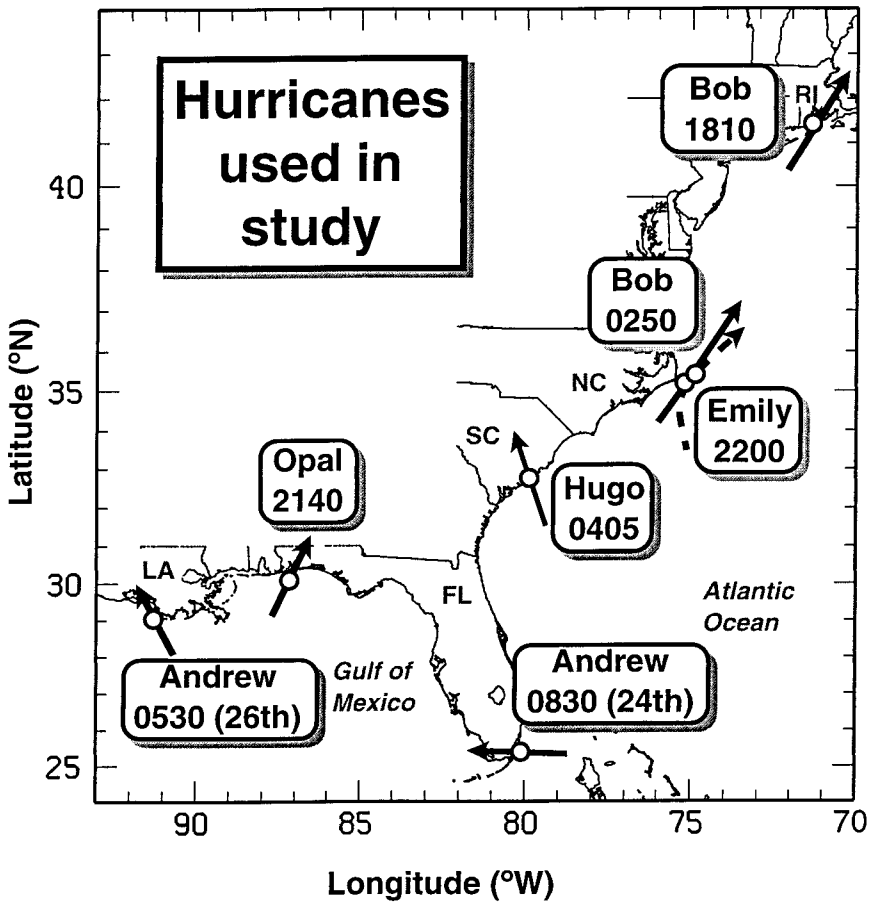

FIG. 1. The location (open circle) and time (UTC) of each hurricane used in this study. Track segments with arrows indicate the direction of motion of each hurricane (Emily's track segment is dashed to distinguish it from Bob's near NC and Andrew's landfill dates are shown).

The circulation center of the SLOSH model parametric wind field is the geometric center of the eye regardless of the hurricane's forward motion. When the storm is at rest, the circulation center and geometric center of the storm are theoretically in the same location (i.e., if one ignores convection and other influences). Once the hurricane has forward motion, the air in the original calm geometric center moves at the storm speed. The result is that the calm portion of the eye shifts to the left (when facing the direction of a hurricane's forward motion). Therefore, the snapshot of the SLOSH model's circulation center may vary slightly from the one used in the HRD wind fields. For comparisons made between the SLOSH and HRD winds, the center of circulation was assumed to be the midpoint between their centers.

TABLE 1. Reference for the storm history of each hurricane used in the study.

Hurricane	Storm history
Hugo (1989)	Case and Mayfield (1990)
Bob (1991)	Pasch and Avila (1992)
Andrew (1992)	Mayfield et al. (1994)
Emily (1993)	Pasch and Rappaport (1995)
Opal (1995)	Lawrence et al. (1998)

b. HRD surface wind fields

HRD's surface wind fields were based on all available surface wind observations from buoys, Coastal–Marine Automated Network platforms, ships, and other surface facilities. Because these data are often sparse near hurricanes, aircraft flight-level observations [adjusted to the surface with a planetary boundary layer model (Powell 1980)] were used to supplement the in situ surface measurements. The method used to create comprehensive datasets conforming to a common framework for exposure, height, and averaging time was described by Powell et al. (1996). These data were then objectively analyzed with a technique based upon the spectral application of finite element representation (SAFER) method (Ooyama 1987; DeMaria et al. 1992; Franklin et al. 1993). The resulting gridded wind fields have estimated errors of 10%–20%, compared to errors of 20%–40% if procedures are not followed to provide a com-

TABLE 2. Parameters input into SLOSH in each hurricane ''snapshot'' at landfall by state is listed with the time, date, pressure deficit (Δp), radius of maximum wind (R_{MW}), translation speed (V_t), and heading.

Hurricane	Landfall state	Time (UTC)	Date	Δp (kPa)	R_{MW} (km)	V_t (m s^{-1})	Heading (°)
Hugo	SC	0405	22 Sep 1989	7.6	46.0	12.3	330
Bob	NC	0250	19 Aug 1991	5.4	38.0	9.8	25
Bob	RI	1810	19 Aug 1991	4.6	62.8	16.1	35
Andrew	FL	0830	24 Aug 1992	8.7	14.5	8.0	275
Andrew	LA	0530	26 Aug 1992	6.5	37.0	4.9	325
Emily	NC	2200	31 Aug 1993	5.2	43.0	5.1	15
Opal	FL	2140	04 Oct 1995	6.4	86.0	10.3	20

mon observation framework (Powell et al. 1996). Since Hurricane Emily (Burpee et al. 1994), HRD surface wind fields have been provided to hurricane specialists at NHC on a real-time experimental basis as guidance for wind radii (17.5, 25, and 33 m s^{-1}) issued in tropical cyclone advisories. Nearly 100 real-time surface wind analyses were provided to NHC for the Atlantic basin each hurricane season from 1995 to 1998.

Since the surface data collection network was sparse, surface observations were collected over an extended time interval prior to landfall, which ranged from 3 h in Emily to 7 h for Hurricanes Hugo and Bob (Table 3). These observations were transformed to a hurricane-centered coordinate system for analysis. Implicit in this analysis was the assumption of invariant storm intensity during the data collection period. This assumption was considered valid prior to landfall, since the largest changes in intensities observed in these storms usually occurred after the eye crossed the coastline.

For oceanographic modeling, wind speed averaging times of at least 10 min are normally considered to be representative of timescales associated with oceanic response to surface stress. The SLOSH model wind speeds are considered equivalent to 10-min means (Jelesnianski et al. 1992; Houston and Powell 1994). For comparison purposes, the HRD mesoscale analysis winds (V_{MESO}) were adjusted to produce maximum 10-min sustained winds using a gust factor relationship (G_{10}) described by Houston and Powell (1994). The resulting winds were maximum 10-min sustained, 10-m marine surface winds (V_{M10}).

Each hurricane's analysis domain was centered on the storm near the time of its closest approach to the coastline and the time ranges of the data input to the analysis were included in Table 3. The analysis filter wavelength [λ defined by Powell et al. (1996)] acted as a low-pass filter to reduce observational noise associated with exposure and sampling differences, including small-scale wind features (e.g., turbulent and convective gusts and lulls) that cannot be adequately resolved by the available observations. The values were also chosen to allow the resolution of mesoscale features, such as the vortex and rainband wind maxima. Because of the smoothing inherent in the objective analysis scheme, a method of amplitude restoration was applied to the V_{MESO} located at radii within $1.5R_{MW}$ to ensure that the maximum 10-min sustained wind was contained in the final analysis output field. The values of λ in Table 3 were chosen to minimize the smoothing of the observed peak wind speed by the SAFER method and ranged from 12.2 km for Andrew's south Florida landfall to 28.9 km for Bob's landfall in New England. As an example, a λ of 22 km and a V_{MESO} of 36 m s^{-1} would result in a timescale of over 20 min (i.e., $t = 2\lambda \div V_{MESO}$). Hence, V_{M10} over a 20-min period would be 2% higher (i.e., $G_{10} = 1.02$) than V_{MESO}, or 36.7 m s^{-1}.

The sensitivity of the SAFER method to the distribution of wind observations and its ability to reproduce a known or model-generated wind field is discussed in the appendix. These tests indicated that the data coverage was adequate in each case and the SAFER technique correctly reproduced *known* surface wind fields based on the available wind observations.

3. Comparisons of SLOSH and observation-based wind fields

Gridpoint differences between HRD's observation-based wind fields and SLOSH wind fields (hereafter

TABLE 3. Wavelength and time range (beginning and ending hours) for the data used to create the V_{HRD} winds for each hurricane landfall.

Hurricane	Landfall state	Wavelength (km)	Begin (UTC)	End (UTC)
Hugo	SC	16.7	2200 (21 Sep)	0500 (22 Sep)
Bob	NC	16.7	2300 (18 Aug)	0600 (19 Aug)
Bob	RI	28.9	1615	2120
Andrew	FL	12.2	0410	1030
Andrew	LA	22.2	0300	0830
Emily	NC	27.8	2030	2330
Opal	FL	21.1	2040 (4 Oct)	0300 (5 Oct)

referred to as V_{HRD} and V_{SLOSH}, respectively) were examined using the methods described in the appendix. In this case, the V_{SLOSH} at each grid point was subtracted from the V_{HRD} at the corresponding grid point. The same grid spacing was used and the statistics for the normalized wind speed difference [NWSD; i.e., $(V_{HRD} - V_{SLOSH}) \div V_{HRD}$] and inflow angle difference (IAD) will be examined at the end of this section.

a. Hurricane Hugo (1989)

Hurricane Hugo's 6.1-m maximum storm surge in the Bulls Bay area of South Carolina (Case and Mayfield 1990) agreed closely with the peak SLOSH-computed storm surge (NOAA 1990). For the Hurricane Hugo V_{HRD}, the aircraft flight-level data above 3 km were adjusted to the surface as described by Powell et al. (1991). The V_{HRD} greater than 50 m s^{-1} covered a large area extending from Bulls Bay into the Atlantic Ocean (Fig. 2a), which closely agreed with the area of V_{SLOSH} speeds greater than 50 m s^{-1} (Fig. 2b) and the location of the peak surge along the coast. The peak V_{SLOSH} speed was 3 m s^{-1} less than the peak V_{HRD} speed (Table 4). The V_{SLOSH} speeds near the northern South Carolina coast decreased more rapidly beyond $1.5R_{MW}$ than the V_{HRD} speeds.

The largest variations in the NWSD field (Fig. 2c) occurred in the rear of the storm where the V_{SLOSH} speeds were over 30% stronger, while the differences were less than 10% in the vicinity of the eyewall near Bulls Bay. The V_{HRD} speeds over the northern South Carolina coast were from 10% to 20% greater than the V_{SLOSH} speeds. SLOSH-computed storm surges values were also less than the observed high-water levels along the coast of northern South Carolina over 100 km from the storm center (NOAA 1990). This underestimate was likely due to the combination of weaker V_{SLOSH} in the region and the lack of wave effects in the model. The IADs (Fig. 2d) ranged from $-10°$ to $-20°$ near Bulls Bay, indicating that the V_{HRD} had greater inflow than the V_{SLOSH} in the peak wind region. IADs were mostly negative throughout the domain with the V_{HRD} having 40° more inflow in the rear of the storm. Insufficient inflow does not appear to be significant for peak storm surge computations, but might be important for computing water-level time series and wave computations that consider ocean currents and the direction of wave motion.

b. Hurricanes Bob (1991) and Emily (1993) near North Carolina

Hurricanes Bob and Emily both passed near Diamond Shoals east of the North Carolina coast (Fig. 1). Hurricane Bob made landfall in Rhode Island 15 h after passing offshore from North Carolina, while Emily later turned out to sea.

1) HURRICANE BOB

The V_{HRD} for Hurricane Bob early on 19 August 1991 during its closest approach to Cape Hatteras, North Carolina (Fig. 3a), depicted the highest wind speeds to the right of the storm (Bob was moving north-northeast). The V_{SLOSH} speeds were ~10% greater than V_{HRD} speeds near the location of peak winds (>45 m s^{-1}), while the peak V_{SLOSH} and V_{HRD} speeds were nearly the same (Table 4). Beyond the area of peak winds, V_{HRD} speeds (Fig. 3a) decreased less with increasing radius, resulting in speeds 10%–40% larger than the V_{SLOSH} speeds (Fig. 3b). The V_{SLOSH} in the vicinity of Cape Hatteras over Pamlico Sound, which were lake winds, were at least 40% weaker than the V_{HRD}. Despite these large differences, the observed and SLOSH-computed storm surges for the North Carolina Outer Banks (including the Pamlico Sound side where the R_{MW} on the left side of Bob was east of Cape Hatteras) were nearly the same. The IADs (Fig. 3d) indicated that V_{SLOSH} inflow angles were 10°–20° larger than the V_{HRD} inflow angles on the north side of the storm (Fig. 3d) and up to 40° less near the rear of the storm's core.

The peak SLOSH-computed storm surges (based on the parametric wind field) were close to the observed surges along the North Carolina coast in this case. However, because the V_{SLOSH} were lower than the V_{HRD} well east of Bob's center, a wave model using the V_{SLOSH} as input would likely underestimate the height of large oceanic waves generated east of Bob.

2) HURRICANE EMILY

Peak V_{HRD} speeds in Emily (Fig. 4a) were nearly the same strength to the left and right of the northward-moving storm during its closest approach to Cape Hatteras (Burpee et al. 1994). The V_{HRD} were approximately northerly at speeds greater than 40 m s^{-1} over most of eastern Pamlico Sound (Fig. 4a). The peak V_{HRD} speed for Emily was more than 7 m s^{-1} greater than the peak V_{SLOSH} speed (Table 4) and Fig. 4b indicates the area of strongest V_{SLOSH} speeds was located to the right of the storm center (again, the V_{SLOSH} over Pamlico Sound were lake winds). The V_{SLOSH} speeds were from 30% to 40% less than the V_{HRD} speeds over both coasts of the Outer Banks (Fig. 4c). The IADs (Fig. 4d) indicated that V_{SLOSH} inflows were very weak throughout most of the eyewall region.

The strong winds in Emily's western eyewall over the shallow waters of Pamlico Sound and the nearly 90° angle shape of the sound's shoreline near Cape Hatteras resulted in an observed peak storm surge (~3.4 m) nearly twice the SLOSH-computed storm surge (Pasch and Rappaport 1995). Only by setting SLOSH input parameters to unrealistic values could V_{SLOSH} be increased over Pamlico Sound. However, this would likely result in overprediction of wind speeds (and accompanying surge and waves) on the right side of Emily.

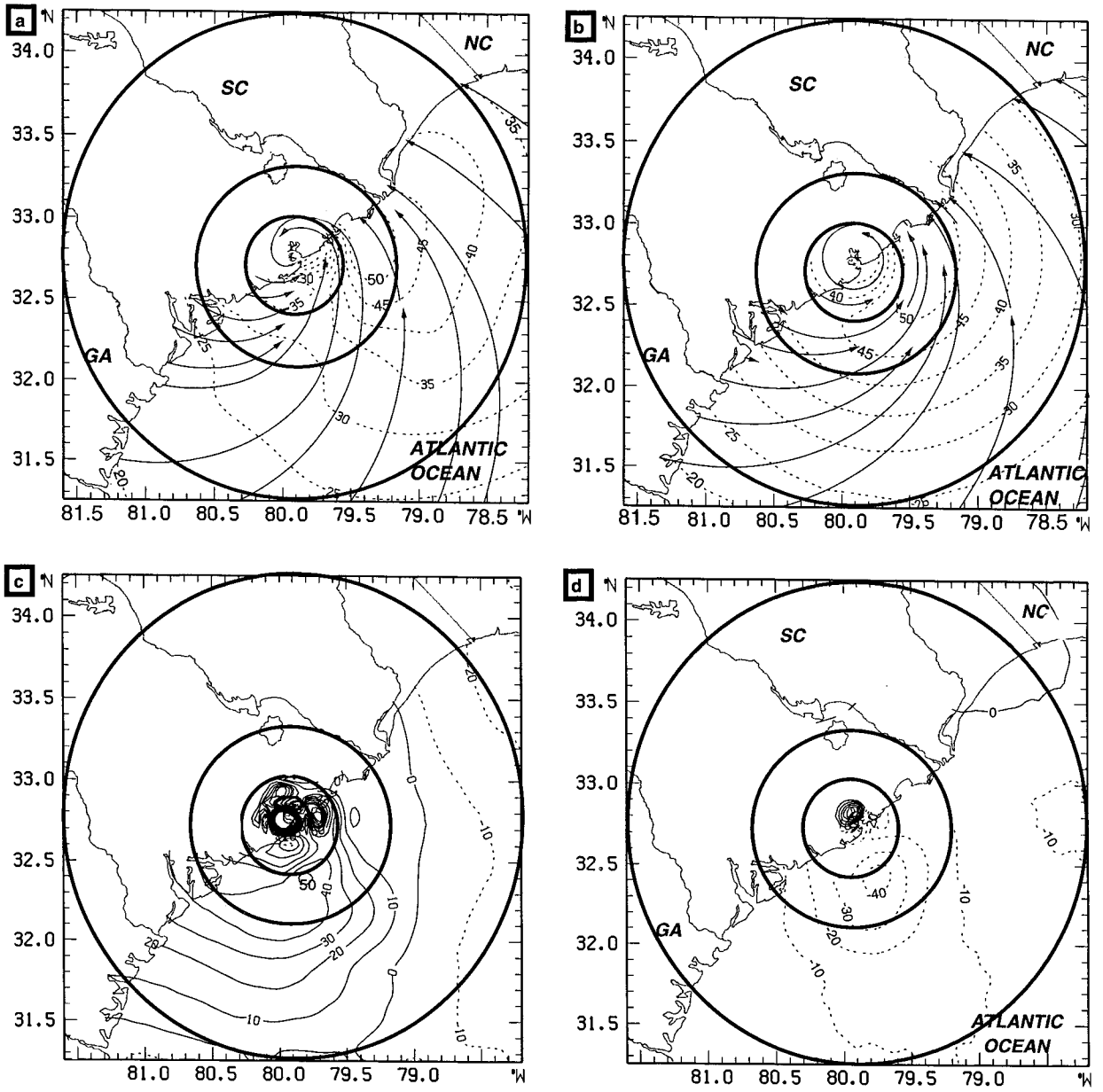

FIG. 2. Wind fields over water for Hurricane Hugo at 0405 UTC 22 Sep 1989. The winds are displayed as streamline and isotachs (units of wind speed are m s^{-1}). The range rings are $0.75R_{MW}$ (inner), $1.50R_{MW}$ (middle), and 158 km (outer) from the storm center. The winds in (a) are the V_{HRD} and the winds in (b) are the V_{SLOSH}. The difference fields are (c) the NWSD field (%) and (d) the IAD (°) where dashed contours are negative.

TABLE 4. The peak V_{HRD} and V_{SLOSH} wind speeds for each hurricane landfall.

Hurricane	V_{HRD} (m s^{-1})	V_{SLOSH} (m s^{-1})
Hugo	57.7	54.4
Bob (NC)	46.4	46.1
Bob (RI)	41.2	41.0
Andrew (FL)	60.9	63.1
Andrew (LA)	50.6	48.9
Emily	49.3	41.9
Opal	42.8	42.0

c. Hurricane Andrew (1992)

The V_{HRD}, V_{SLOSH}, SLOSH-computed storm surges, and the observed high-water marks for Hurricane Andrew's landfall near Homestead, Florida, at 0830 UTC 24 August 1992 were discussed in PH96. Peak V_{SLOSH} speeds north of the eye were 2–3 m s^{-1} higher than the V_{HRD} speeds, but covered a much larger portion of the eyewall and were located closer to the storm center. Peak V_{SLOSH} speeds near the southern eyewall were about 10 m s^{-1} larger than the V_{HRD} speeds. The computed

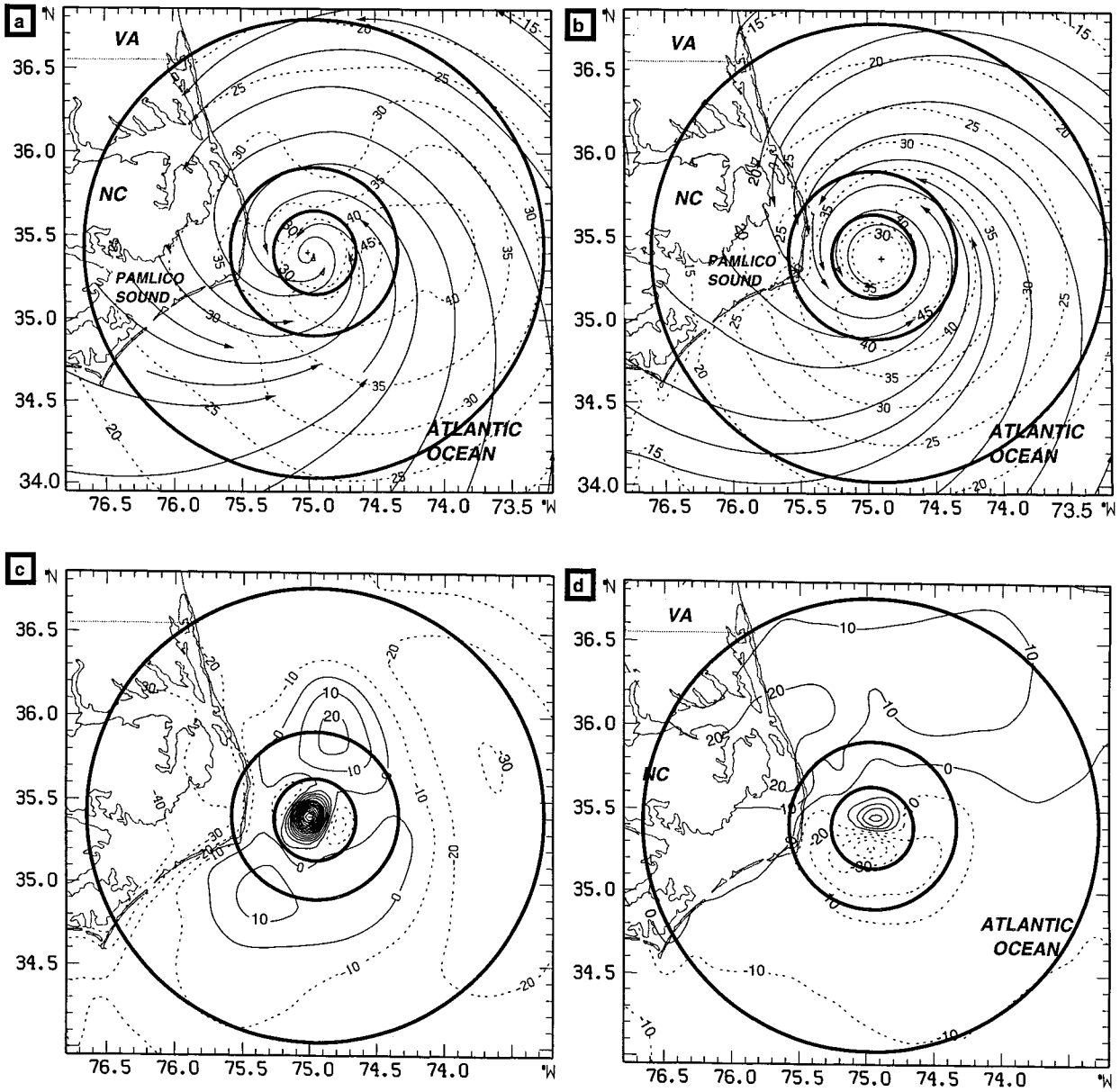

FIG. 3. Same as Fig. 2 except for Hurricane Bob at 0250 UTC 19 Aug 1991 and the outer radius was 153 km.

SLOSH storm surges were slightly less than the observed peak, but values to the north were 1–1.5 m higher than the measured values. The underestimate of the peak surge may have been a result of using lake winds over all of Biscayne Bay and the lack of wave effects in the model.

d. Hurricane Opal (1995)

Hurricane Opal was a category 4 hurricane based on the Saffir–Simpson scale (Saffir 1977; Simpson and Riehl 1981) less than 12 h prior to landfall in the Florida panhandle (Lawrence et al. 1998). Opal weakened to near the lower threshold of category 3 strength at landfall with a very asymmetric wind field (Powell and Houston 1998). Opal's strong wind speeds while it was a category 4 hurricane produced very high waves over the Gulf of Mexico [e.g., a significant wave height of 8.3 m was observed at National Data Buoy Center (NDBC) buoy 42001 on the left side of Opal during the hurricane's closest approach to the buoy]. These waves later arrived at the Florida panhandle beaches where the bottom topography offshore, coastal relief, shape of the coastline, and storm surge resulted in very large measured-outside high-water marks (B. Jarvinen, TPC, 1996, personal communication). The storm surges

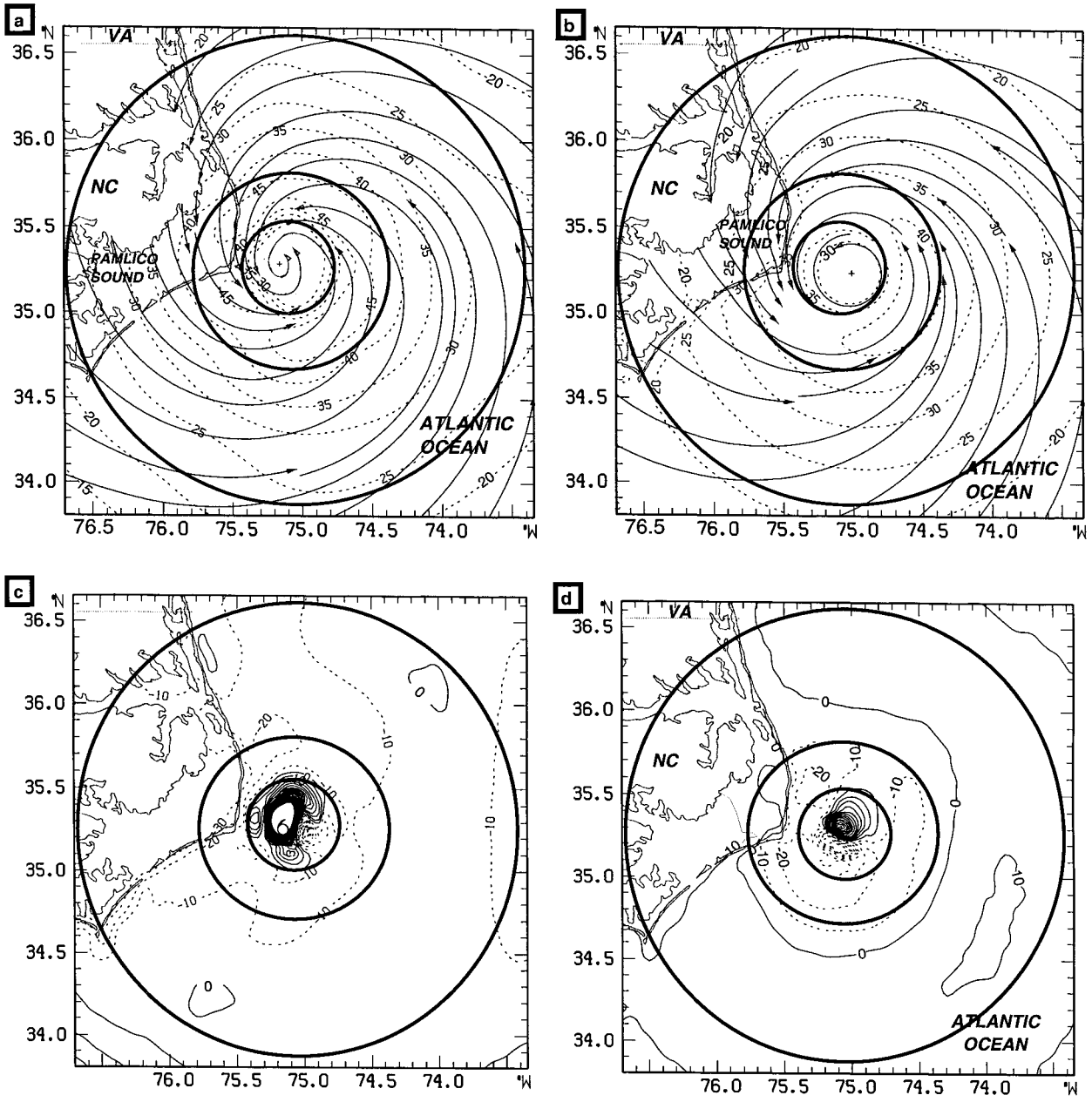

FIG. 4. Same as Fig. 2 except for Hurricane Emily at 2200 UTC 31 Aug 1993 and the outer radius was 150 km.

(without waves) recorded by tide gauges in the area were close to the SLOSH-computed storm surges. There was only a small area of over 40 m s^{-1} speeds in the V_{HRD} to the right of the northward moving storm at landfall (Fig. 5a). Opal's V_{SLOSH} (Fig. 5b) contained a large area of over 40 m s^{-1} speeds east of the storm center. The area of V_{HRD} speeds over 40 m s^{-1} was much larger prior to landfall at 1830 UTC (Fig. 5c).

e. Statistics for difference fields

Gridpoint differences between the V_{SLOSH} and V_{HRD} were examined for all seven cases. In Table 5, statistics for all grid points at radii ranging from $0.75R_{MW}$ to $1.50R_{MW}$ were used to determine variations in the vicinities of hurricanes that have the highest winds, largest storm surges, and the largest waves. The V_{SLOSH} speeds were greater than the V_{HRD} speeds (i.e., NWSD were positive) in all cases, except for Emily, which had a mean (μ) of -16%. The NWSD values of μ for the other hurricanes ranged from $+3\%$ for Bob (NC) to $+29\%$ for Bob (RI). Negative IADs confirm that the V_{HRD} have between 11° and 25° more inflow than V_{SLOSH} within the region of highest winds.

Although the peak surge, winds, and waves are not

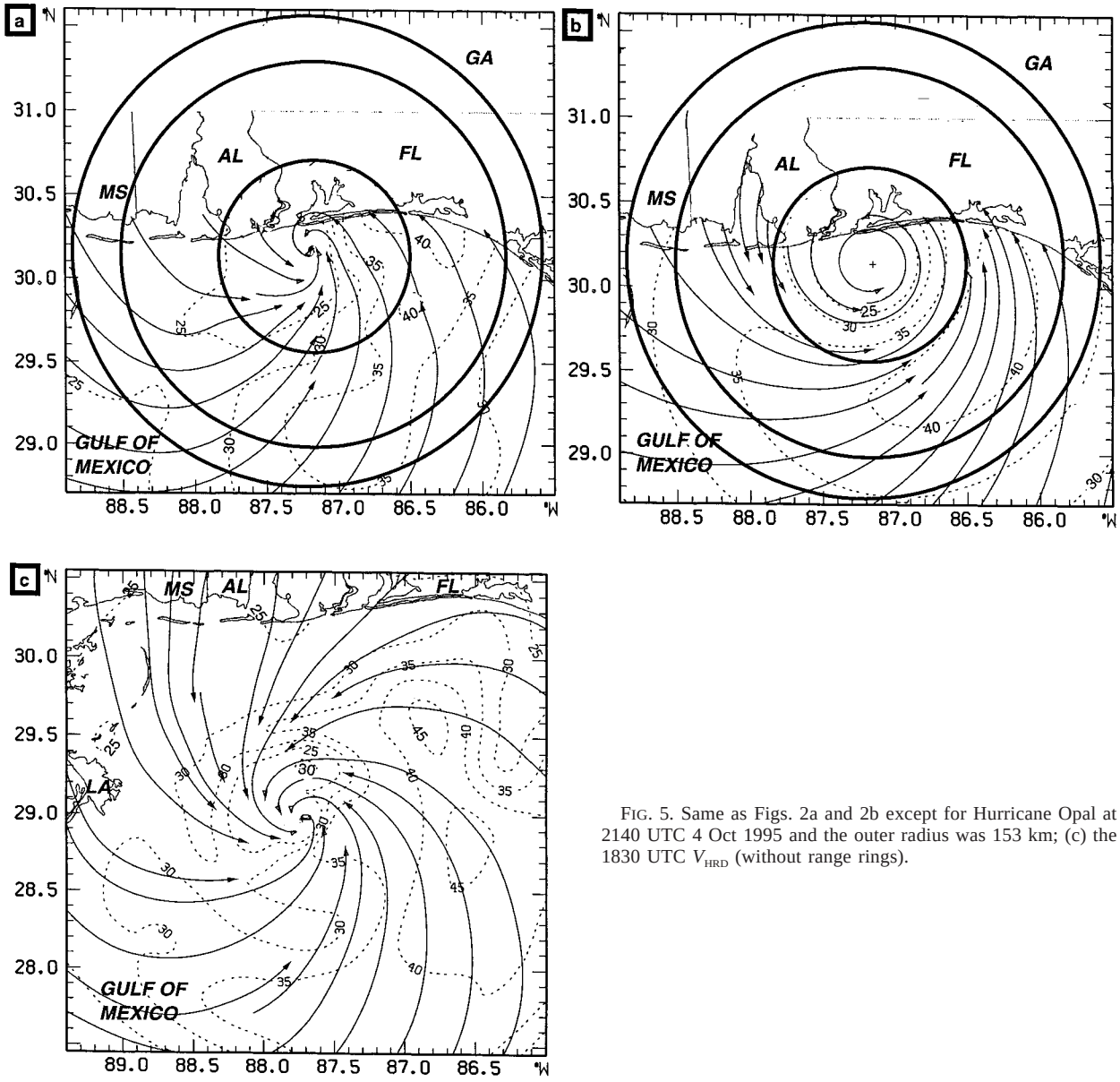

FIG. 5. Same as Figs. 2a and 2b except for Hurricane Opal at 2140 UTC 4 Oct 1995 and the outer radius was 153 km; (c) the 1830 UTC V_{HRD} (without range rings).

TABLE 5. Statistics [means and standard deviations (shown in parentheses)] for NWSD and IAD for radii over water from 0.75 R_{MW} to 1.50 R_{MW}.

Hurricane	Vicinity	n	NWSD (%)	IAD (°)
Hugo		203	+24 (18)	−24 (10)
Bob	NC	302	+3 (9)	−11 (12)
Bob	RI	354	+29 (15)	−22 (12)
Andrew	FL	50	+10 (9)	−17 (7)
Andrew	LA	198	+19 (13)	−14 (8)
Emily		389	−16 (10)	−12 (7)
Opal		841	+18 (12)	−25 (13)
All cases		2337	+14 (18)	−19 (13)

contained in the outer region of the storm (radius $> 1.5R_{MW}$), damaging storm effects still occur here. In Table 6, the V_{HRD} for Bob (NC) and Emily were 15% and 10%, respectively, larger than the V_{SLOSH} in the outer region. The V_{SLOSH} were from 3% to 27% greater than the V_{HRD} for the other five cases. The magnitudes of the IAD for the V_{SLOSH} and V_{HRD} in the outer region were less than 10° for all seven cases.

4. SLOSH hindcasts in Emily and Opal using V_{HRD}

The V_{HRD} from Emily and Opal were put into SLOSH to test the feasibility of making storm surge computations using observation-based wind fields. Opal's broad wind field and large R_{MW} prior to and during landfall

TABLE 6. Same as Table 5 except for radii from 1.50 R_{MW} to the outer radius.

Hurricane	n	NWSD (%)	IAD (°)
Hugo	1208	+5 (17)	−9 (6)
Bob (NC)	2217	−15 (13)	+1 (10)
Bob (RI)	1045	+27 (17)	−3 (9)
Andrew (FL)	543	+3 (10)	−5 (13)
Andrew (LA)	857	+20 (13)	−3 (9)
Emily	1958	−10 (8)	+5 (5)
Opal	411	+16 (10)	−9 (9)
All cases	8239	+1 (20)	−1 (10)

(Powell and Houston 1998) indicated large asymmetries and the strongest winds were primarily located on the right-hand side of the storm as it moved rapidly northward (Figs. 5a and 5c). Also, Opal's track was nearly perpendicular to the coastline at landfall (Fig. 1). In contrast, Hurricane Emily's slow forward motion and distribution of eyewall convection resulted in a nearly symmetric surface wind field [see Fig. 4a and Burpee et al. (1994)] with very strong winds over Pamlico Sound as the hurricane traveled northward nearly parallel to the coast east of Cape Hatteras.

The V_{HRD} were input into the SLOSH model to compute maximum surges by assuming the wind and surface pressure fields were steady state for 28 h in Emily and 30 h for Opal. This required a redesign of SLOSH to use a full nonparametric invariant hurricane wind field as input (note that the use of time-varying V_{HRD} as input would require a time-interpolation scheme for SLOSH to allow for input at intervals as small as 1 h). The steady-state assumption was reasonable for Hurricane Emily (Fig. 4a), but Hurricane Opal was rapidly weakening prior to landfall, invalidating the invariant wind field assumption in this case. The 1830 UTC V_{HRD} was used for Opal, since it was considered more representative of the hurricane as it moved over the continental shelf prior to landfall.

SLOSH model runs with the V_{HRD} and V_{SLOSH} for Opal at landfall (Fig. 6) showed good agreement. The largest storm surge for the V_{HRD} was ~2.9 m, but it was displaced nearly 40 km closer to Opal's track than the SLOSH-computed peak surge height. This likely reflects the stronger winds in the HRD wind fields nearer the center. The model-computed storm surges compared well to the observed values at three tide gauges at the coast.

For Emily, the oceanic V_{SLOSH} over eastern Pamlico Sound near Cape Hatteras were at least 10 m s^{-1} weaker than the V_{HRD} speeds (Fig. 7), resulting in the peak computed storm surge at Cape Hatteras being 1.2 m less than the observed. The peak storm surge computed using the V_{HRD} in SLOSH was only 0.4 m less than the observed.

5. Discussion and conclusions

In general, SLOSH wind fields were very similar to the HRD observation-based wind fields in the region of

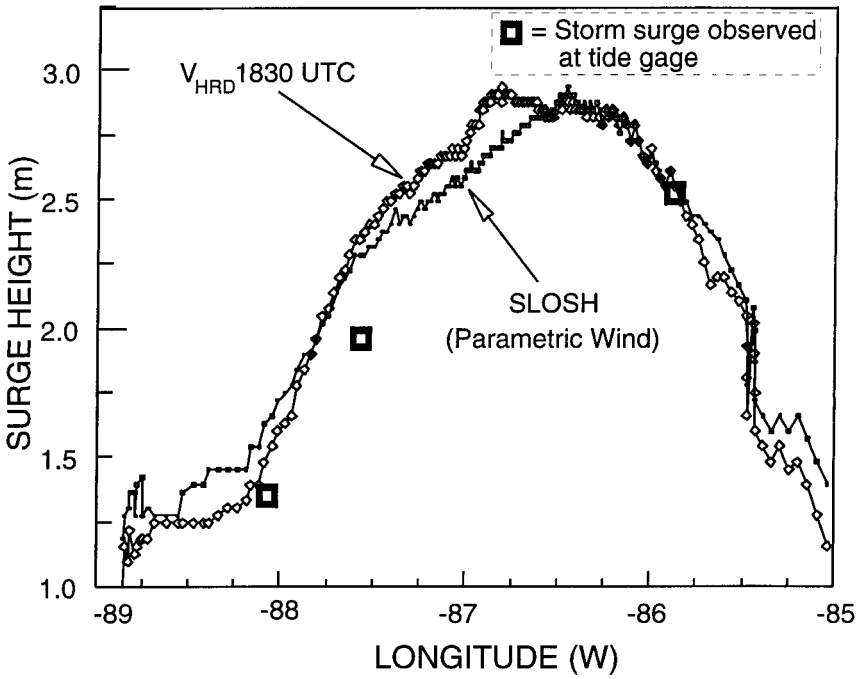

FIG. 6. Hurricane Opal's computed peak storm surges along the Gulf Coast between 85° and 89°W longitude using the V_{SLOSH} and V_{HRD} (1830 UTC) winds as input. The observed peak storm surges from tide gauges (large open squares) in the area of Opal's landfall are shown.

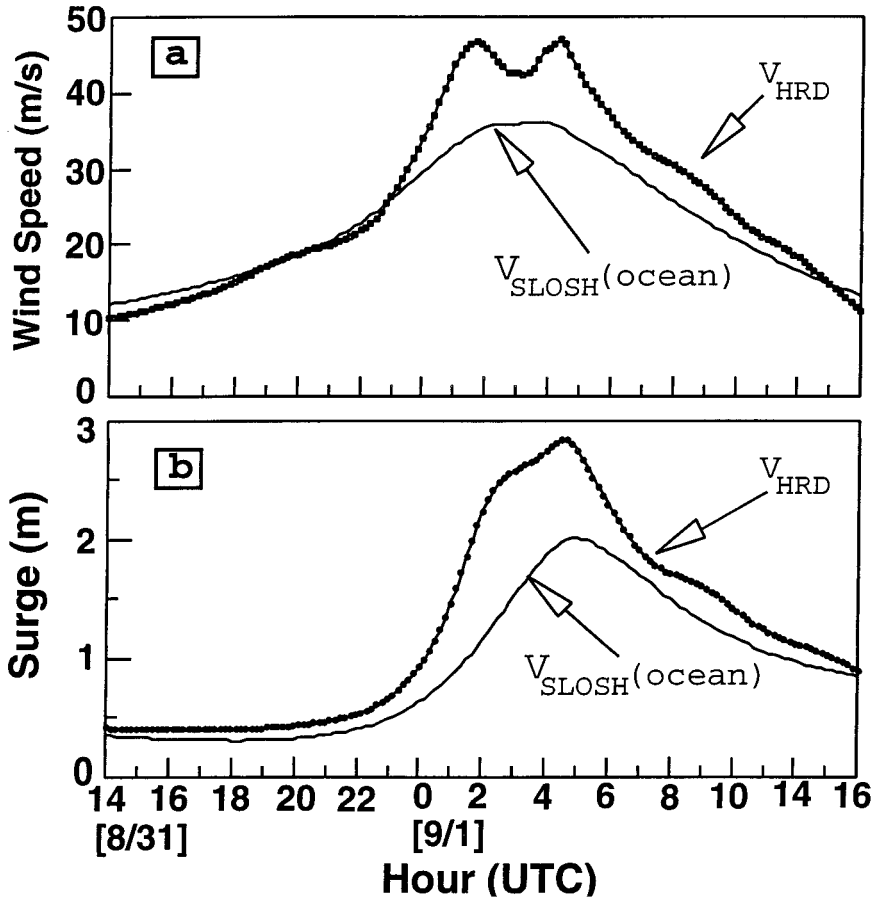

FIG. 7. Time series of (a) Hurricane Emily's V_{SLOSH} (ocean) and V_{HRD} (2200 UTC) and storm surge from 1400 UTC 31 Aug to 1600 UTC 1 Sep 1993 wind speeds (m s^{-1}) and (b) computed peak storm surge values on the Pamlico Sound side of Cape Hatteras, NC.

the highest winds for six of the seven hurricane cases studied. Two regions of winds were considered when computing statistics for the differences between the V_{SLOSH} and V_{HRD} for all seven cases: an inner region containing radii ranging from $0.75R_{MW}$ to $1.50R_{MW}$ and an outer region containing radii ranging from $1.50R_{MW}$ to an outer radius (which was based on the size of each storm's domain). In the inner region, the SLOSH wind speeds were an average of 14% greater than the V_{HRD} speeds and the mean inflow angles for SLOSH averaged 19° less than the V_{HRD} inflow angles. The mean differences for the wind speeds and inflow angles in the outer region were −1% and +1°, respectively.

Hurricane Emily was a major exception since the V_{SLOSH} speeds were much weaker than V_{HRD} speeds in the inner region. This underestimate resulted in a peak SLOSH-computed storm surge over Pamlico Sound that was only one-half of the observed height. Emily's symmetric wind structure was influenced by strong convection on the left side of the storm (Burpee et al. 1994).

For Andrew's landfall in south Florida, the observed high-water marks in the Cutler Ridge area south of Miami were underestimated approximately 0.5 m by SLOSH, while the SLOSH-computed surges to the north of the peak were overestimated by over 1.0 m (PH96). The weaker V_{SLOSH} over portions of Biscayne Bay (lake winds) may account for some of the differences in the area of the peak surge in Cutler Ridge, which has a mostly open exposure from the Atlantic Ocean for easterly winds (note that not being able to include wave effects in SLOSH computations may have also contributed to the underestimate of the computed peak storm surge here). Discerning overwater versus overland trajectories, if included, may have potentially improved the SLOSH model computations for Andrew's landfall in south Florida. The V_{SLOSH} lake winds that were flowing from Miami Beach and Key Biscayne southwestward across Biscayne Bay would change to an oceanic trajectory in the location of the observed peak storm surge as the winds shifted to a more easterly direction. Determining flow trajectories may improve the accuracy of SLOSH-computed storm surge near the observed maximum water marks in this case. Other SLOSH basins may benefit from local trajectory distinctions in certain

scenarios of landfalling hurricanes (e.g., Tampa and Galveston Bays).

Differences between the V_{HRD} and V_{SLOSH} for the hurricane wind fields examined were shown to have been generally small near the R_{MW} in most cases, but the differences often increased at radii beyond the region of peak winds. For example, in the Bulls Bay area of South Carolina, the V_{HRD} and V_{SLOSH} were relatively close and the observed high-water marks and SLOSH-computed storm surges were nearly the same in Hurricane Hugo. However, the V_{SLOSH} were weaker than V_{HRD} to the northeast of the center at outer radii; hence, the SLOSH-computed storm surge decreased more rapidly than the observed surges along the northern South Carolina coast 100 km northeast of the storm center (the inclusion of waves in SLOSH could conceivably have improved the computed storm surges here).

For Opal, the SLOSH model storm surge computations matched well with the water levels observed by tide gauges in the area. Wave setup and runup added to the surge resulted in debris line high-water marks more than twice as large as the tide gauge measurements and SLOSH-computed storm surges. The V_{SLOSH} were sometimes less than the V_{HRD} wind fields for outer wind radii according to Table 6, especially in Hurricanes Bob (NC) and Emily. The V_{SLOSH} inflow angles in the inner core were less than the V_{HRD} inflow angles, but show little difference in the outer region. Future versions of the SLOSH model, which might contain computations of wave heights, directions, and oceanic currents, would likely be sensitive to wind direction errors.

The large differences between surge measurements and high-water marks point to the need for future models to incorporate both surge and waves. Possible augmentation of the current SLOSH model to include wave effects (e.g., wave setup, wave runup, etc.) is under investigation. Despite significant improvements in wave modeling technologies during the last 10 years [Dr. Robert Jensen, Coastal Hydraulic Laboratory/U.S. Army Corps of Engineers (USACE), 1997, personal communication], hurricane wave simulation and validation studies have been limited because of the lack of high-resolution wind fields and directional wave data for verification. These problems make it difficult to distinguish whether absolute errors in wave height computation were caused by wave model deficiency or inherent errors in the winds.

The SLOSH parametric model uses a simple wind model, designed for use in an operational forecasting environment. The model gives a good representation of hurricane surface winds, based on minimal input and is recommended when observations are insufficient to define the wind field. Real-time operational storm surge predictions for coastal areas threatened by landfall rely on forecasts of the storm's track, intensity (central pressure), size (R_{MW}), and outer wind characteristics, which are all subject to large errors. The use of observation-based winds in SLOSH would likely be most beneficial during and immediately after a hurricane landfall, especially in cases known to challenge parametric models. Some examples include 1) Hurricane Emily, which had intense convection on the left side according to Burpee et al. (1994); 2) Hurricane Bob, which showed the effects of fast forward motion, especially evident on the left and left-rear portion of the storm's circulation (these effects are mostly observed north of 30°N latitude); 3) major hurricanes with concentric eyewalls such as Allen (1980) and Gilbert (1988) described by Willoughby et al. (1982); 4) storms influenced by strong environmental vertical wind shear [e.g., Hurricane Norbert (1984) described by Marks et al. (1992)]; 5) cases in northern latitudes where the hurricane's circulation causes warm air advection over cold water bodies resulting in a stably stratified boundary layer (Powell and Black 1990); and 6) cases with rapid intensification where the inner core and outer wind radii respond differently (provided data coverage and timeliness are sufficient to document such changes).

An accurate diagnosis of storm surge flooding, based on observation-based wind fields, can be supplied to emergency management agencies and government officials responsible for identifying areas requiring search and rescue and to identify damages to transportation, communication, and utility systems.

The wind fields produced in real time and after the fact by HRD are now being made available on a Web site (http://www.aoml.noaa.gov/hrd) for researchers to use in comparisons with model output or with remote wind sensing platforms (e.g., Special Sensor Microwave/Imager and the Second European Remote Sensing Satellite). Tests of the feasibility of using real-time HRD surface winds in the SLOSH model for landfalling hurricanes are currently being planned for future hurricane seasons (possibly in 1999).

Acknowledgments. B. Jarvinen (TPC) provided some input parameters used for SLOSH and the observed storm surges for Hurricane Opal. C. Bakker and L. Amat (HRD) developed software for data visualization. J. Franklin and S. Feuer (HRD) assisted with the surface wind analyses. R. Kohler (HRD) and R. St. Fleur (MAST Academy) assisted with the display of gridded wind fields. Special thanks to these dedicated crews for providing flight-level data, which were essential for producing the HRD surface wind fields: the 53d Weather Squadron of the U.S. Air Force Reserves and the NOAA Aircraft Operations Center. Other essential meteorological observations were provided by NOS, NWS (including the NDBC and the National Climatic Data Center), and the Department of Defense. High-water marks were provided by the U.S. Geological Survey and USACE (with funding from FEMA). S. Rogers (NC Sea Grant) provided additional observations in Hurricane Opal. Reviews of the manuscript by V. Wiggert and J. Cione of HRD and two anonymous reviewers were extremely helpful.

APPENDIX

Sensitivity Tests for the HRD Winds

It was decided that a method for testing the adequacy of the data coverage and evaluating the amplitude restoration used to generate the V_{HRD} was necessary for each of the cases examined here. In addition, a determination of which regions of the hurricane's domain (i.e., near the maximum winds and beyond) should be used to make statistical comparisons between the V_{HRD} and V_{SLOSH} was needed. Because the SLOSH parametric wind model computes wind speed and direction at every point in the hurricane's domain, these model winds were used as the basis for the tests.

In the first sensitivity test for the HRD analysis method, the known or model-generated wind field was created for each of the seven landfall cases using the SLOSH parametric wind model to define a wind everywhere in the domain. The SLOSH winds were then linearly interpolated at actual observation locations to create a set of synthetic wind observations for each case (e.g., in Hurricane Bob shown in Fig. A1). The SAFER method was then applied to the synthetic observations and amplitude restoration was used on the synthetic

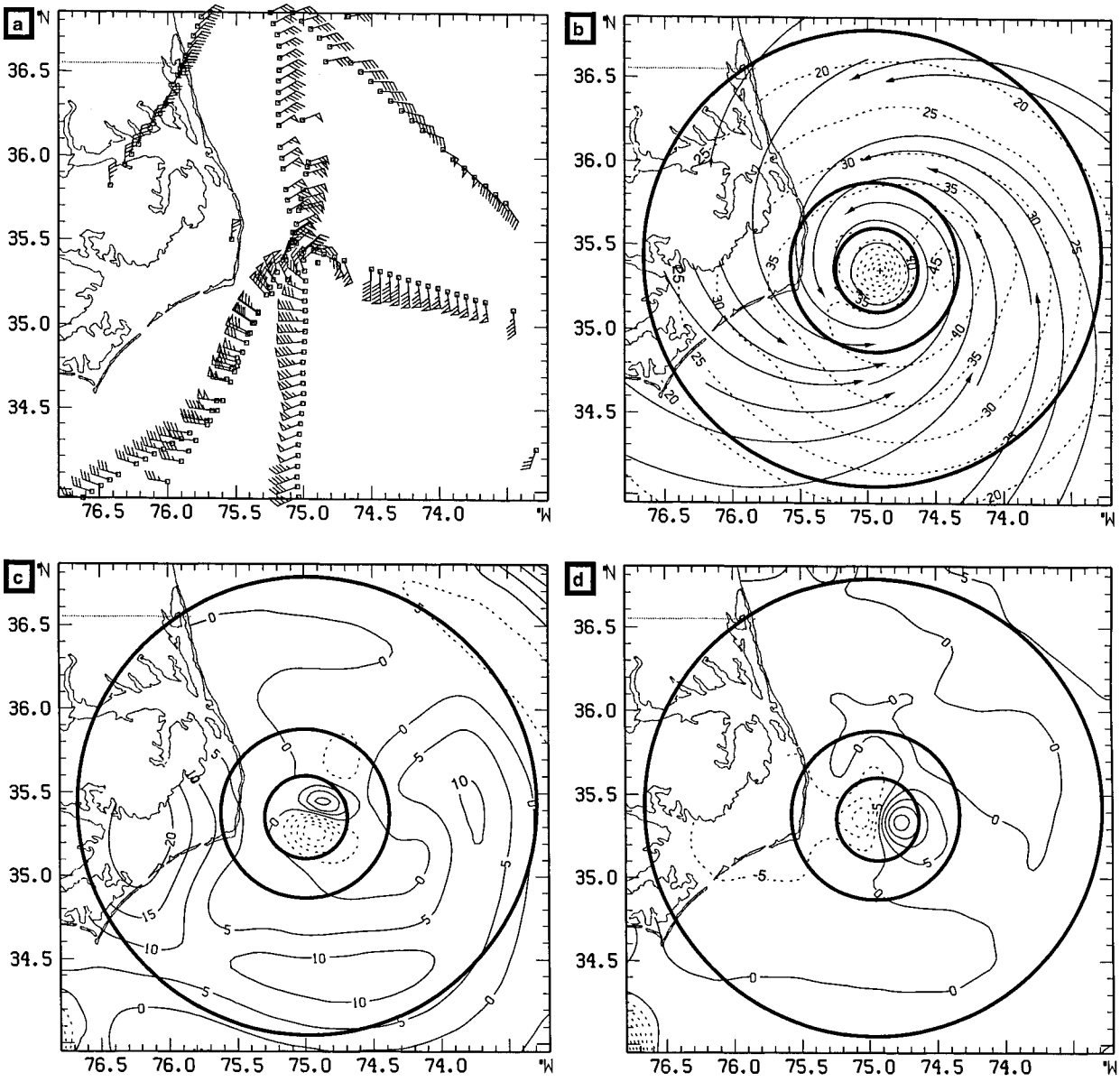

FIG. A1. Synthetic winds for Hurricane Bob at 0250 UTC 19 Aug 1991 where (a) shows the synthetic wind barbs used to compute the (b) V_{SYN} (isotachs and streamlines), (c) NWSD (%), and (d) IAD (°).

TABLE A1. Sensitivity test with means and standard deviations (shown in parentheses) for V_{SYN} minus known winds. The NWSD and IAD are shown for radii over water from 0.75 R_{MW} to 1.50 R_{MW}.

Hurricane	n	0.75 R_{MW} (km)	1.50 R_{MW} (km)	NWSD (%)	IAD (°)
Hugo	203	34.5	69.0	+1 (2)	+2 (2)
Bob (NC)	302	28.5	57.0	0 (4)	0 (5)
Bob (RI)	354	47.3	94.5	+1 (2)	+1 (2)
Andrew (FL)	50	10.9	21.8	−3 (3)	0 (1)
Andrew (LA)	198	27.8	55.5	+2 (2)	0 (4)
Emily	389	32.3	64.5	+2 (3)	0 (3)
Opal	841	64.5	129.0	−1 (4)	−1 (2)
All cases	2337			+0.3 (3.5)	+0.2 (2.9)

TABLE A2. Same sensitivity test as in Table A1 except for radii ranging from 1.50 R_{MW} to the outer radius.

Hurricane	n	1.50 R_{MW} (km)	Outer (km)	NWSD (%)	IAD (°)
Hugo	1208	69.0	158.0	+5 (4)	−1 (2)
Bob (NC)	2217	57.0	153.0	+5 (6)	−1 (2)
Bob (RI)	1045	94.5	150.0	−4 (6)	−1 (2)
Andrew (FL)	543	21.8	69.0	+4 (4)	−1 (1)
Andrew (LA)	857	55.5	122.0	+1 (2)	0 (2)
Emily	1958	64.5	150.0	+1 (5)	0 (2)
Opal	411	129.0	153.0	−5 (4)	+1 (2)
All cases	8239			+1.9 (6.0)	−0.4 (1.9)

TABLE A3. Same as Table A1 except for all observed winds minus V_{HRD} for radii over water from 0.75 R_{MW} to 1.50 R_{MW}.

Hurricane	Landfall state	n	0.75 R_{MW} (km)	1.50 R_{MW} (km)	NWSD (%)	IAD (°)
Hugo	SC	24	34.5	69.0	0 (7)	0 (4)
Bob	NC	29	28.5	57.0	0 (6)	+2 (8)
Bob	RI	37	47.3	94.5	−3 (8)	+1 (7)
Andrew	FL	21	10.9	21.8	+4 (10)	0 (5)
Andrew	LA	24	27.8	55.5	+2 (11)	−3 (6)
Emily	NC	42	32.3	64.5	+3 (13)	+1 (11)
Opal	FL	49	64.5	129.0	−1 (5)	0 (3)
All cases		226			+0.4 (9.1)	+0.2 (6.9)

TABLE A4. Same as Table A3 except for radii over water from 1.50 R_{MW} to the outer radius.

Hurricane	Landfall state	n	1.50 R_{MW} (km)	Outer (km)	NWSD (%)	IAD (°)
Hugo	SC	68	69.0	158.0	−5 (10)	+1 (7)
Bob	NC	91	57.0	153.0	−1 (11)	0 (7)
Bob	RI	46	94.5	150.0	−3 (14)	−1 (5)
Andrew	FL	85	21.8	69.0	−3 (12)	0 (6)
Andrew	LA	102	55.5	122.0	+7 (9)	−5 (5)
Emily	NC	80	64.5	150.0	−6 (8)	+1 (6)
Opal	FL	7	129.0	153.0	−5 (10)	0 (3)
All cases		479			−0.2 (13.0)	−0.7 (6.8)

V_{MESO} for radii within 1.5R_{MW}. The result was a wind field based on synthetic observations (V_{SYN}) that could then be compared with the known (i.e., SLOSH in this case) wind field for each hurricane (Fig. A1b). If the two wind fields compared well, the HRD analysis method faithfully reproduced the known wind field.

The analyzed synthetic observations were compared to the known field by computing the difference for wind speeds and inflow angles between the known and V_{SYN} at all grid points. The grid spacing used in each case was 0.5° latitude × 0.5° longitude, except for Hurricane Andrew in south Florida, which had a grid spacing of 0.4° latitude × 0.4° longitude. The wind speed differences at each grid point were divided by the known

TABLE A5. Same as Table A1 except for in situ surface winds only minus V_{HRD} for radii over water from 0.50 R_{MW} to the outer radius.

Hurricane	Landfall state	n	0.50 R_{MW} (km)	Outer (km)	NWSD (%)	IAD (°)
Hugo	SC	9	23.0	158.0	−12 (14)	+11 (10)
Bob	NC	41	19.0	153.0	−4 (13)	+5 (9)
Bob	RI	58	31.4	150.0	−7 (11)	+1 (7)
Andrew	FL	36	7.3	69.0	−7 (14)	+1 (6)
Andrew	LA	0	18.5	122.0	—	—
Emily	NC	37	21.5	150.0	−6 (14)	+3 (12)
Opal	FL	19	43.0	153.0	−4 (7)	0 (2)
All cases		200			−6.0 (13.0)	+2.5 (8.7)

wind speed at the same grid point to produce NWSDs; the IAD were not normalized. Examples of these difference fields for Hurricane Bob are shown in Figs. A1c and A1d.

Differences between the known and V_{SYN} were largest in the vicinity of each hurricane's eye and inner core where gradients were largest. Therefore, error statistics for known and V_{SYN} winds were computed at marine grid points within the following radii: 1) from $0.75R_{MW}$ to $1.50R_{MW}$, which contains the region of the maximum winds for each storm; and 2) the domain beyond $1.50R_{MW}$ (the outer radius ranged from 69 to 158 km and was based on the extent of each storm's analysis domain). In addition, the edges of the domain were excluded to minimize possible effects of any noise that might exist at the boundaries. For inner radii (Table A1), the NWSDs ranged from −3% to +1% with a μ near zero and σ of 3.5%, while the IADs ranged from −1° to +2° with μ also near zero and σ of 3°. The outer annulus (Table A2) NWSD's ranged from −5% to +5% with a μ of +2% (σ = 6%), indicating that the analyzed synthetic wind speeds were slightly stronger on average than the known wind speeds. The IAD μ was slightly negative (σ = 2°). The mean differences (not shown) between known and V_{SYN} radial and tangential winds were near zero in both regions. The storm with the least number of data points within the inner annulus was Andrew (FL), while Opal had the least number of data points in the outer annulus. This did not appear to cause a significant increase in the errors in the V_{SYN}. These statistics indicated that the data coverage was adequate and the SAFER technique correctly reproduced known surface wind fields based on the available wind observations.

Another sensitivity test examined the differences between the V_{HRD} and the data input to the analyses. All observations (including flight-level winds adjusted to the surface) and gridded V_{HRD} fields within the same two sets of radii used in the above test were included (in situ observations minus V_{HRD} were examined here). It was found that for 226 cases, the μ for the NWSD in the inner radii case (Table A3) was near zero, but slightly positive (σ = 9%), and the IAD μ was also near zero (σ = 7°). The outer radii region had 479 comparisons (Table A4), with an NWSD μ near zero (σ = 13%) and the IAD μ was −1° (σ = 7°). This test indicated that the SAFER technique correctly reproduced the wind fields in the vicinity of the actual observations that were used to generate the V_{HRD} fields.

The final sensitivity test used the same technique to examine the differences between only the in situ surface observations and the V_{HRD} (i.e., aircraft observations adjusted to the surface were *not* used in this test). In this case, the limited number of in situ surface observations required that only one range of radii be used to compute the statistics (here the radii were from $0.5R_{MW}$ to the outer radius). The value of NWSDs in Table A5 were negative in all cases with a μ of −6.0% (σ = 13.0%) and the IADs were always positive with a μ of +2.5° (σ = 8.7°). Therefore, the aircraft observations in the SAFER method were in general increasing the HRD wind speeds and the HRD inflow angles were slightly less than the actual observed.

REFERENCES

Burpee, R. W., and Coauthors, 1994: Real-time guidance provided by NOAA's Hurricane Research Division to forecasters during Emily of 1993. *Bull. Amer. Meteor. Soc.*, **75,** 1765–1783.

Case, R., and M. Mayfield, 1990: Atlantic hurricane season of 1989. *Mon. Wea. Rev.*, **118,** 1165–1177.

DeMaria, M., S. M. Aberson, K. V. Ooyama, and S. J. Lord, 1992: A nested spectral hurricane model for hurricane track forecasting. *Mon. Wea. Rev.*, **120,** 1628–1643.

Franklin, J. L., S. J. Lord, S. E. Feuer, and F. D. Marks, 1993: The kinematic structure of Hurricane Gloria (1985) determined from nested analyses of dropwindsonde and Doppler data. *Mon. Wea. Rev.,* **121,** 2433–2451.

Hock, T. R., and J. L. Franklin, 1999: The NCAR GPS dropwindsonde. *Bull Amer. Meteor. Soc.*, **80,** 407–420.

Houston, S. H., and M. D. Powell, 1994: Observed and modeled wind and water-level response from Tropical Storm Marco (1990). *Wea. Forecasting,* **9,** 427–439.

Jarrell, J. D., P. J. Hebert, and M. Mayfield, 1992: Hurricane experience levels of coastal county populations from Texas to Maine. NOAA Tech. Memo. NWS NHC 46, 152 pp. [Available from NOAA/AOML Library, 4301 Rickenbacker Cswy., Miami, FL 33149.]

Jarvinen, B. R., and M. B. Lawrence, 1985: An evaluation of the SLOSH storm surge model. *Bull. Amer. Meteor. Soc.*, **66,** 1408–1411.

Jelesnianski, C. P., J. Chen, and W. A. Shaffer, 1992: SLOSH: Sea, lake, and overland surges from hurricanes. NOAA Tech. Report NWS 48, 71 pp. [Available from NOAA/AOML Library, 4301 Rickenbacker Cswy., Miami, FL 33149.]

Lawrence, M. B., M. Mayfield, L. Avila, R. Pasch, and E. N. Rappaport, 1998: Atlantic hurricane season of 1995. *Mon. Wea. Rev.*, **126,** 1124–1151.

Marks, F. D., Jr., R. H. Houze Jr., and J. F. Gamache, 1992: Dual-aircraft investigation of the inner core of Hurricane Norbert. Part I: Kinematic structure. *J. Atmos. Sci.,* **49,** 919–942.

Mayfield, M., L. A. Avila, and E. N. Rappaport, 1994: Atlantic hurricane season of 1992. *Mon. Wea. Rev.,* **122,** 517–538.

McAdie, C. J., and M. B. Lawrence, 1993: Long-term trends in National Hurricane Center track forecast errors in the Atlantic basin. Preprints, *20th Conf. on Hurricanes and Tropical Meteorology,* San Antonio, TX, Amer. Meteor. Soc., 281–284.

NOAA, 1990: Hurricane Hugo, September 10–22, 1989. U.S. Dept. of Commerce Natural Disaster Survey Rep., NOAA, 61 pp. [Available from NOAA/AOML Library, 4301 Rickenbacker Cswy., Miami, FL 33149.]

Ooyama, K. V., 1987: Scale controlled objective analysis. *Mon. Wea. Rev.,* **115,** 2479–2506.

Pasch, R., and L. Avila, 1992: Atlantic hurricane season of 1991. *Mon. Wea. Rev.,* **120,** 2671–2687.

——, and E. N. Rappaport, 1995: Atlantic hurricane season of 1993. *Mon. Wea. Rev.,* **123,** 871–886.

Powell, M. D., 1980: Evaluations of diagnostic marine boundary layer models applied to hurricanes. *Mon. Wea. Rev.,* **108,** 757–766.

——, and P. G. Black, 1990: The relationship of hurricane reconnaissance flight-level wind measurements to winds measured by NOAA's oceanic platforms. *J. Wind Eng. Indust. Aerodynam.,* **36,** 381–392.

——, and S. H. Houston, 1996: Hurricane Andrew's landfall in south Florida. Part II: Surface wind fields and potential real-time applications. *Wea. Forecasting,* **11,** 329–349.

——, and ——, 1998: Surface wind fields of 1995 Hurricanes Erin, Opal, Luis, Marilyn, and Roxanne at landfall. *Mon. Wea. Rev.,* **126,** 1259–1273.

——, P. P. Dodge, and M. L. Black, 1991: The landfall of Hurricane Hugo in the Carolinas: Surface wind distribution. *Wea. Forecasting,* **6,** 379–399.

——, S. H. Houston, and T. A. Reinhold, 1996: Hurricane Andrew's landfall in south Florida. Part I: Standardizing measurements for documentation of surface wind fields. *Wea. Forecasting,* **11,** 304–328.

Saffir, H. S., 1977: Design and construction requirements for hurricane resistant construction. Preprint No. 2830, ASCE, 20 pp. [Available from American Society of Civil Engineers, New York, NY 10017.]

Simpson, R. H., and H. Riehl, 1981: *The Hurricane and its Impact.* Louisiana State University Press, 398 pp.

Willoughby, H. E., J. A. Clos, and M. G. Shoreibah, 1982: Concentric eyewalls, secondary wind maxima, and the evolution of the hurricane vortex. *J. Atmos. Sci.,* **39,** 395–411.